Dynamic Behaviour of an Elastic Orthotropic Shaft

IOAN PARAUSANU[1]*, ANTON HADAR[1], GIGEL PARASCHIV[2], DANA CODRUTA VISAN[1]

[1]Politehnica University of Bucharest, Faculty of Engineering and Management of Technological Systems, 313 Splaiul Independentei, 060042, Bucharest, Romania

[2] Politehnica University of Bucharest, Faculty for Biotechnical Engineering Systems, 313 Splaiul Independentei, 060042, Bucharest, Romania

The dynamic behaviour of an orthotropic shaft leads to a nonlinear differential equation, Mathieu type, whose solving is quite difficult. Certain problems in theoretical physics lead to Mathieu equation, particularly the problem of the propagation of electromagnetic waves in a medium with a periodic structure, the problem of the electrons' motion in a crystal lattice in the quantum theory of metals. The parametric equation was solved numerically for time history and was time integrated using Runge-Kutta method with initial boundary values. The results show a totally different dynamic behaviour of the shaft made of an orthotropic material compared with the one made of an isotropic material.

Key-words: orthotropic material, shaft, orbit precession motion

It is well-known that a composite material is a material made from two or more constituent materials with significantly different physical or chemical properties that, when combined, produce a material with characteristics that differ from the individual components. The individual components remain separate and distinct within the finished structure [1].

The physical properties of composite materials are generally not isotropic (independent of direction of applied force) in nature, but rather are typically anisotropic (different depending on the direction of the applied force or load). For instance, the stiffness of a composite panel will often depend upon the orientation of the applied forces and/or moments. Panel stiffness is also dependent on the design of the panel (for instance: the fiber reinforcement and matrix used, the method of panel built, type of weave and orientation of fiber axis to the primary force). In contrast, isotropic materials in standard wrought forms, typically have the same stiffness regardless of the directional orientation of the applied forces and/or moments.

The relationship between forces/moments and strains/curvatures for an isotropic material can be described with the following material properties: Young's Modulus, the shear Modulus and the Poisson's ratio, in relatively simple mathematical relationships [2]. For the anisotropic material, it requires the mathematics of a second order tensor and up to 21 material property constants. For the special case of orthogonal isotropy, there are three different material property constants for each of Young's Modulus, Shear Modulus and Poisson's ratio, a total of 9 constants to describe the relationship between forces/moments and strains/curvatures.

Advanced composite materials have unique mechanical properties compared to steel, including fatigue strength, specific strength (ratio of strength to weight), specific rigidity (ratio of modulus of elasticity to weight), strength redundancy and high resistance of damaged structures to external loads. In contrast to metals, the crack resistance of modern composite materials increases as strength increases. The crack resistance of composite materials depends on fiber tensile strength, matrix tensile strength and bond shear strength. Fiber content is defined by studying the cross-section of a specimen. The parameter is equal to the ration of the total area of the unidirectional fiber to the cross-sectional area of the specimen. Regarding fiber reinforced matrices, the modulus of elasticity will increase with larger hard fiber content [3].

In this paper a shaft made of an unidirectional composite material, reinforced with carbon fiber, is considered. In the cross-section of the shaft there are two different Young's Modulus, corresponding to two orthogonal directions. The dynamic behaviour of an unidirectional composite material shaft was studied in order to find out the differences between this one and the classical steel shaft.

Mathematical model of an elastic orthotropic shaft

Taking into account the fact that the composites tend to replace more and more the classical materials, so the existing models do not correspond from the static and dynamic point of view due to the modification of the properties of the materials, it becomes necessary to find new models to describe as well as possible the behaviour of structures.

In a static behaviour the things are simpler, they are more complicated in the dynamic one, and especially in the case of a shaft made of an orthotropic material and set in a rotation motion. The orthotropy of the material from which the shaft is made, is due to the longitudinal reinforcement with fibres whose layout leads to getting of different elastic properties, related to two perpendicular axes. The shaft, presented in figure 1, was considered to be at rest. If, a force F acts perpendicularly on the axis of the shaft, a linear desplacement on the force direction will appear in a certain section. If the shaft has the diameter d and the force is situated midway between the bearings, where l is the irrespective distance, also knowing the longitudinal elasticity module of the material E, the displacement δ, at the midlle of the shaft, will be [4]:

$$\delta = \frac{Fl^3}{48EI} \quad (1)$$

where $I = \pi d^4 / 64$ represents the moment of inertia of the cross section of the shaft. Further, consider a shaft made of an orthotropic material, which, in cross-section, has different modules of elasticity $E_u \neq E_v$. The frame XOY is a fixed one, while the frame UOV is a rotating one, having a rotational movement at the constant speed of the shaft. At time $t = 0$ the force F coincides with the OV axis, resulting the arrow δ_v, then, after the shaft has rotated by 90°, the force F, which keeps its direction, will coincide with the

* email: ioan.parausanu@upb.ro

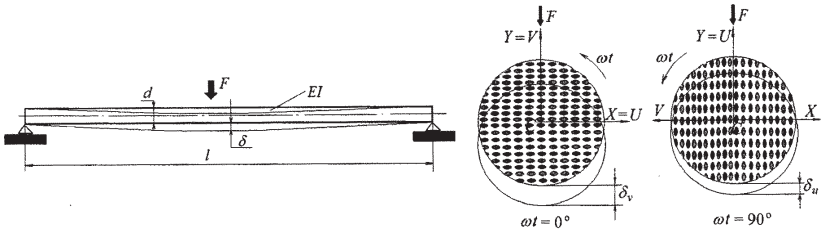

Fig. 1. The orthotropic shaft and its cross section

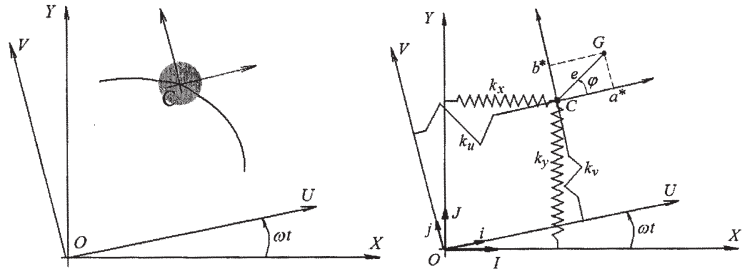

Fig. 2. The two frames of the model

OU axis, and the arrow will be δ_u (fig. 1-b). Corresponding to the two arrows, the elastic constants of the shaft on the two directions are:

$$k_u = \frac{48E_u I}{l^3}$$
$$k_v = \frac{48E_v I}{l^3} \quad (2)$$

The shaft shown in figure 1, with circular section, made of an orthotropic material, for which $E_u \neq E_v$ and its geometric centre being the point *C*, executes a precession motion around of the bearings axis with the angular velocity ω. In relation to two frames, one fixed *XOY* and a rotating one *UOV*, the shaft shows different stiffnesses: k_x, k_y and k_u, k_v (fig. 2).

At middistance between the bearings, there is a disk with the mass *m*, that is attached to the shaft. The geometric centre of the cross section of the shaft, the point *C*, coincides with the centre of the rotating frame and, in relation to the fixed frame, it has the coordinates *x* and *y*, and in relation to the rotating one the coordinates *u* and *v*. Between the vectors of the axes of the two frames there is the following relation:

$$\begin{bmatrix} \bar{i} \\ \bar{j} \end{bmatrix} = \begin{bmatrix} \cos\omega t & \sin\omega t \\ -\sin\omega t & \cos\omega t \end{bmatrix} \cdot \begin{bmatrix} \bar{I} \\ \bar{J} \end{bmatrix} \quad (3)$$

Considering the mass *m* concentrated in the centre of gravity, point *G*, which is at the distance *e* (eccentricity) towards the geometric centre, its speed is:

$$v_G = \frac{\mathrm{d}\overline{OG}}{\mathrm{d}t} \quad (4)$$

where:

$$\overline{OG} = \overline{OC} + \overline{CG} = [x + e\cos(\omega t + \varphi)] \cdot \bar{I} + [y + e\sin(\omega t + \varphi)] \cdot \bar{J} = (u + a^*) \cdot \bar{i} + (v + b^*) \cdot \bar{j} \quad (5)$$

Taking into account the relationships (3), (4) and (5) and using the writing in the matriceal form, it results:

$$\bar{v}_G = \bar{v}_x + \bar{v}_y = [\dot{x} - e\omega\sin(\omega t + \varphi) \quad \dot{y} + e\omega\cos(\omega t + \varphi)] \cdot \begin{bmatrix} \bar{I} \\ \bar{J} \end{bmatrix} =$$
$$= [\dot{x} - e\omega\sin(\omega t + \varphi) \quad \dot{y} + e\omega\cos(\omega t + \varphi)] \cdot \begin{bmatrix} \cos\omega t & -\sin\omega t \\ \sin\omega t & \cos\omega t \end{bmatrix} \cdot \begin{bmatrix} \bar{i} \\ \bar{j} \end{bmatrix} =$$
$$= \begin{bmatrix} \dot{x}\cos\omega t + \dot{y}\sin\omega t - e\omega\cos^2\omega t\sin\varphi - e\omega\sin^2\omega t\sin\varphi \\ -\dot{x}\sin\omega t + \dot{y}\cos\omega t + e\omega\sin^2\omega t\cos\varphi + e\omega\cos^2\omega t\cos\varphi \end{bmatrix} \cdot \begin{bmatrix} \bar{i} \\ \bar{j} \end{bmatrix} \quad (6)$$

But:

$$\begin{bmatrix} u \\ v \end{bmatrix} = \begin{bmatrix} \cos\omega t & \sin\omega t \\ -\sin\omega t & \cos\omega t \end{bmatrix} \begin{bmatrix} x \\ y \end{bmatrix} \quad (7)$$

So:

$$\begin{bmatrix} \dot{u} \\ \dot{v} \end{bmatrix} = \begin{bmatrix} \dot{x}\cos\omega t + \dot{y}\sin\omega t + \omega v \\ -\dot{x}\sin\omega t + \dot{y}\cos\omega t - \omega u \end{bmatrix} \quad (8)$$

From (8) result:

$$\dot{x}\cos\omega t + \dot{y}\sin\omega t = \dot{u} - \omega v$$
$$-\dot{x}\sin\omega t + \dot{y}\cos\omega t = \dot{v} + \omega u \quad (9)$$

Introducing the relationship (9) into (6) we get:

$$\bar{v}_G = \bar{v}_x + \bar{v}_y = \begin{bmatrix} \dot{u} - \omega v - \omega a\sin\varphi \\ \dot{v} + \omega u + \omega a\cos\varphi \end{bmatrix} \cdot \begin{bmatrix} \bar{i} \\ \bar{j} \end{bmatrix} = \begin{bmatrix} \dot{u} - \omega(v + b^*) \\ \dot{v} + \omega(u + a^*) \end{bmatrix} \cdot \begin{bmatrix} \bar{i} \\ \bar{j} \end{bmatrix} \quad (10)$$

So, the speed of the point *G* was expressed both in relationship with the fixed frame (the first part of the relationship (6)), and in relationship with the rotating frame (the last part of the relationship (10)).

Taking into account that $v_G^2 = v_x^2 + v_y^2$, one can express the kinetic energy $T = mv_G^2/2$ of the mass *m*, concentrated in the point *G*, both in relationship with the fixed reference system – the relation (11), and depending on the mobile one – the relation (12).

$$T = \frac{m}{2}\left[\dot{x}^2 + \dot{y}^2 + e^2\omega^2 - 2e\omega\dot{x}\sin(\omega t + \varphi) + 2e\omega\dot{y}\cos(\omega t + \varphi)\right] \quad (11)$$

$$T = \frac{m}{2}\left[\dot{u}^2 - 2\dot{u}v\omega - 2\dot{u}b^*\omega + \omega^2v^2 + 2\omega^2vb^* + \omega^2(b^*)^2 + \right.$$
$$\left. + \dot{v}^2 + 2\dot{v}u\omega + 2\dot{v}a^*\omega + \omega^2u^2 + 2\omega^2ua^* + \omega^2(a^*)^2\right] \quad (12)$$

Using Lagrange, for the fixed reference system is obtained:

$$\frac{\mathrm{d}}{\mathrm{d}t}\left(\frac{\partial T}{\partial \dot{x}}\right) - \frac{\partial T}{\partial x} = m\ddot{x} - me\omega^2\cos(\omega t + \varphi)$$
$$\frac{\mathrm{d}}{\mathrm{d}t}\left(\frac{\partial T}{\partial \dot{y}}\right) - \frac{\partial T}{\partial y} = m\ddot{y} - me\omega^2\sin(\omega t + \varphi) \quad (13)$$

and for the mobile reference system:

$$\frac{\mathrm{d}}{\mathrm{d}t}\left(\frac{\partial T}{\partial \dot{u}}\right)-\frac{\partial T}{\partial u}=m\left(\ddot{u}-2\dot{v}\omega-\omega^2u-\omega^2a^*\right)$$
$$\frac{\mathrm{d}}{\mathrm{d}t}\left(\frac{\partial T}{\partial \dot{v}}\right)-\frac{\partial T}{\partial v}=m\left(\ddot{v}+2\dot{u}\omega-\omega^2v-\omega^2b^*\right) \quad (14)$$

Forces acting on the mass m are both the gravitational forces F_g and the elastic forces F_e caused by the deformed shaft. They can be expressed in every reference system apart:

$$F_g^f=F_x\bar{I}+F_y\bar{J}=\begin{bmatrix}0 & -mg\end{bmatrix}\cdot\begin{bmatrix}\bar{I}\\ \bar{J}\end{bmatrix} \quad (15)$$

$$F_g^m=\begin{bmatrix}0 & -mg\end{bmatrix}\cdot\begin{bmatrix}\cos\omega t & -\sin\omega t\\ \sin\omega t & \cos\omega t\end{bmatrix}\cdot\begin{bmatrix}\bar{i}\\ \bar{j}\end{bmatrix}=\begin{bmatrix}-mg\sin\omega t & -mg\cos\omega t\end{bmatrix}\cdot\begin{bmatrix}\bar{i}\\ \bar{j}\end{bmatrix} \quad (16)$$

$$F_e^m=\begin{bmatrix}-k_uu & -k_vv\end{bmatrix}\cdot\begin{bmatrix}\bar{i}\\ \bar{j}\end{bmatrix} \quad (17)$$

$$F_e^f=\begin{bmatrix}-k_uu & -k_vv\end{bmatrix}\cdot\begin{bmatrix}\cos\omega t & \sin\omega t\\ -\sin\omega t & \cos\omega t\end{bmatrix}\cdot\begin{bmatrix}\bar{I}\\ \bar{J}\end{bmatrix}=$$
$$=\begin{bmatrix}u & v\end{bmatrix}\cdot\begin{bmatrix}-k_u & 0\\ 0 & -k_v\end{bmatrix}\cdot\begin{bmatrix}\cos\omega t & \sin\omega t\\ -\sin\omega t & \cos\omega t\end{bmatrix}\cdot\begin{bmatrix}\bar{I}\\ \bar{J}\end{bmatrix} \quad (18)$$

If we transpose the relation (7) we will get:

$$\begin{bmatrix}u & v\end{bmatrix}=\begin{bmatrix}x & y\end{bmatrix}\cdot\begin{bmatrix}\cos\omega t & -\sin\omega t\\ \sin\omega t & \cos\omega t\end{bmatrix} \quad (19)$$

Substituting (19) in (18), the elastic force results in the fixed frame:

$$F_e^f=\begin{bmatrix}A & B\end{bmatrix}\cdot\begin{bmatrix}\bar{I}\\ \bar{J}\end{bmatrix} \quad (20)$$

where

$$A=-\frac{1}{2}\left[(k_u+k_v)x+(k_u-k_v)y\sin 2\omega t+(k_u-k_v)x\cos 2\omega t\right]$$
$$B=-\frac{1}{2}\left[(k_u+k_v)y+(k_u-k_v)x\sin 2\omega t-(k_u-k_v)y\cos 2\omega t\right] \quad (21)$$

Neglecting the damping of the bearings and considering them as isotropic ones, with the value k, the forces of the bearings F_b can be expressed in the two reference systems (fixed - f and mobile - m):

$$\bar{F}_b^f=\begin{bmatrix}-kx & -ky\end{bmatrix}\cdot\begin{bmatrix}\bar{I}\\ \bar{J}\end{bmatrix}$$
$$\bar{F}_b^m=\begin{bmatrix}-ku & -kv\end{bmatrix}\cdot\begin{bmatrix}\bar{i}\\ \bar{j}\end{bmatrix} \quad (22)$$

We note with:

$$k_1=\frac{k_u+k_v}{2}+k$$
$$k_2=\frac{k_u-k_v}{2} \quad (23)$$

and taking into account the relation (13) to (17), (20) and (22), the equations of motion of the centre of the shaft in a matriceal form are:

- for the fixed reference system

$$\begin{bmatrix}m & 0\\ 0 & m\end{bmatrix}\cdot\begin{bmatrix}\ddot{x}\\ \ddot{y}\end{bmatrix}+\begin{bmatrix}k_1 & 0\\ 0 & k_2\end{bmatrix}\cdot\begin{bmatrix}x\\ y\end{bmatrix}+\sin 2\omega t\begin{bmatrix}0 & k_2\\ k_2 & 0\end{bmatrix}\begin{bmatrix}x\\ y\end{bmatrix}+$$
$$+\cos 2\omega t\begin{bmatrix}k_2 & 0\\ 0 & -k_2\end{bmatrix}\begin{bmatrix}x\\ y\end{bmatrix}=\begin{bmatrix}0\\ -mg\end{bmatrix}+me\omega^2\begin{bmatrix}\cos(\omega t+\varphi)\\ \sin(\omega t+\varphi)\end{bmatrix} \quad (24)$$

- for the mobile reference system

$$\begin{bmatrix}m & 0\\ 0 & m\end{bmatrix}\cdot\begin{bmatrix}\ddot{u}\\ \ddot{v}\end{bmatrix}+2\omega\begin{bmatrix}0 & -m\\ m & 0\end{bmatrix}\cdot\begin{bmatrix}\dot{u}\\ \dot{v}\end{bmatrix}+\begin{bmatrix}k+k_u-m\omega^2 & 0\\ 0 & k+k_v-m\omega^2\end{bmatrix}\cdot\begin{bmatrix}u\\ v\end{bmatrix}=$$
$$=\begin{bmatrix}me\omega^2\cos\varphi\\ me\omega^2\sin\varphi\end{bmatrix}-mg\begin{bmatrix}\sin\omega t\\ \cos\omega t\end{bmatrix} \quad (25)$$

Solving the equations of motion

Equation (24) describes the nonlinear behaviour of the precession motion of the shaft, made of an orthotropic material, to a fixed reference system. It is a nonlinear differential equation, Mathieu type, whose solving is difficult and many prefer using the equation (25), for which there are known mathematical solutions. The relatively easy solving of the equation (25) shows the disadvantage that the solutions found are in relationship with the mobile reference system, which rotates in the same time with the shaft, and does not offer, under the circumstances, a clear picture of the absolute precession movement, but a relative one. In this article, we tried to find the solutions of the equation (24) and this has been made possible by the numerical methods for solving of this equation, by the Runge-Kutta method. Firstly, the equation (24) was written in a undimensional form, making the following substitution:

$$\omega t=z \quad (26)$$

from where it results:

$$\dot{x}=\frac{\mathrm{d}x}{\mathrm{d}t}=\omega\frac{\mathrm{d}x}{\mathrm{d}z};\quad \ddot{x}=\frac{\mathrm{d}^2x}{\mathrm{d}t^2}=\omega^2\frac{\mathrm{d}^2x}{\mathrm{d}z^2}$$
$$\dot{y}=\frac{\mathrm{d}y}{\mathrm{d}t}=\omega\frac{\mathrm{d}y}{\mathrm{d}z};\quad \ddot{y}=\frac{\mathrm{d}^2y}{\mathrm{d}t^2}=\omega^2\frac{\mathrm{d}^2y}{\mathrm{d}z^2} \quad (27)$$

Now we have four unknowns, the displacements and the velocities corresponding to the two axes of the fixed system of reference and they are described by the vector:

$$\begin{bmatrix}x & y & \frac{\mathrm{d}x}{\mathrm{d}z} & \frac{\mathrm{d}y}{\mathrm{d}z}\end{bmatrix}^{\mathrm{T}} \quad (28)$$

Taking into account (26), (27) and (28), equation (24) can be put in the form:

$$\frac{\mathrm{d}}{\mathrm{d}z}\begin{bmatrix}x\\ y\\ \frac{\mathrm{d}x}{\mathrm{d}z}\\ \frac{\mathrm{d}y}{\mathrm{d}z}\end{bmatrix}=\begin{bmatrix}\frac{\mathrm{d}x}{\mathrm{d}z}\\ \frac{\mathrm{d}y}{\mathrm{d}z}\\ -\frac{k_1+k_2\cos(2z)}{m\omega^2}x-\frac{k_2\sin(2z)}{m\omega^2}y+e\cos(z)\\ -\frac{k_2\sin(2z)}{m\omega^2}x-\frac{k_1-k_2\cos(2z)}{m\omega^2}y-\frac{g}{\omega^2}+e\sin(z)\end{bmatrix} \quad (29)$$

Equation (29) is a second order differential equation with periodic coefficients, whose solution by Runge-Kutta method requires knowing the initial value, at the moment $t = 0$, of the four unknown given by (28). Numerical solution was done in MATLAB, in which a cod based on relation (29) was written, and where, among others, we used the functions DEVAL and ODE45.

The instability of the system

It is well known that the Mathieu equations have both stable and unstable solutions depending on the values of

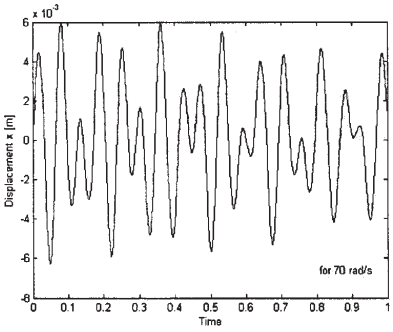

a)

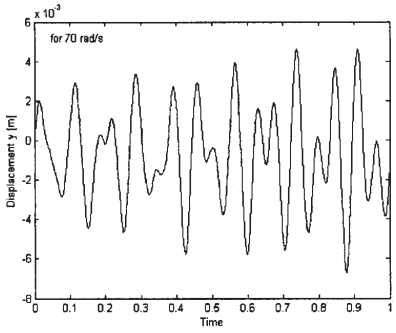

b)

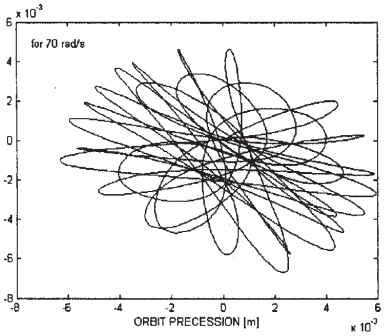

c)

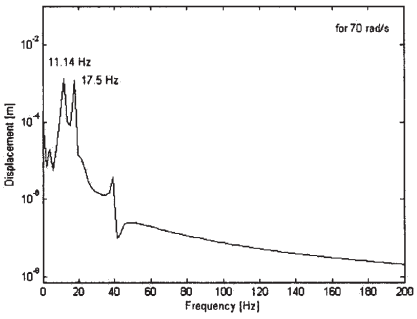

d)

Fig. 3. The simulation results obtained for ω = 70 rad/s compared to the fixed frame

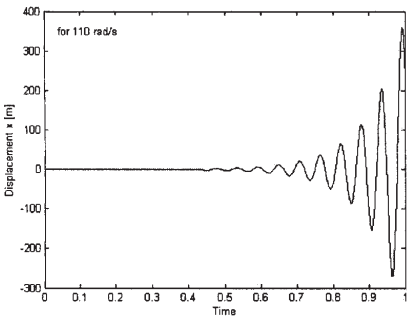

a)

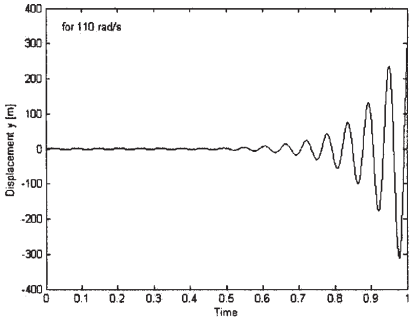

b)

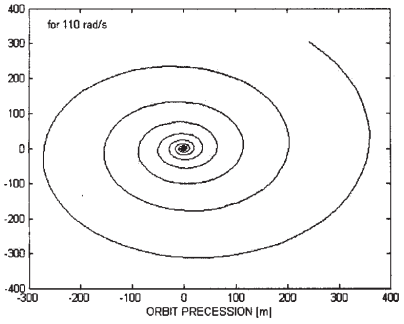

c)

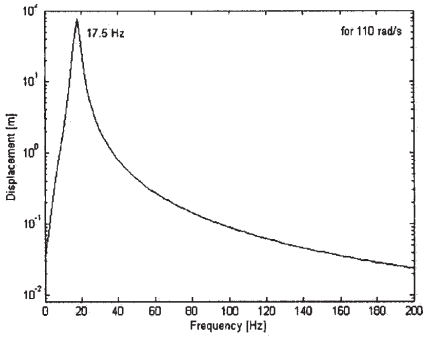

d)

Fig. 4. The simulation results obtained for ω = 110 rad/s compared to the fixed frame

the equation coefficients. To study the instability of the system described by the above equations were the terms on the right side of equation (25) are considered null, a situation that corresponds to a vertical rotor (g = 0) and perfectly balanced (e = 0), so this corresponds to free vibration:

$$\begin{bmatrix} m & 0 \\ 0 & m \end{bmatrix} \cdot \begin{bmatrix} \ddot{u} \\ \ddot{v} \end{bmatrix} + 2\omega \cdot \begin{bmatrix} 0 & -m \\ m & 0 \end{bmatrix} \cdot \begin{bmatrix} \dot{u} \\ \dot{v} \end{bmatrix} + \begin{bmatrix} k + k_u - m\omega^2 & 0 \\ 0 & k + k_v - m\omega^2 \end{bmatrix} \cdot \begin{bmatrix} u \\ v \end{bmatrix} = \begin{bmatrix} 0 \\ 0 \end{bmatrix} \quad (30)$$

Equation (30) has solutions of the form:

$$u = u_0 e^{rt}$$
$$v = v_0 e^{rt} \quad (31)$$

Which, substituted in (30), leads to the following characteristic equation:

$$r^4 + \left(\omega_u^2 + \omega_v^2 + 2\omega^2\right) r^2 + \left(\omega_u^2 - \omega^2\right)\left(\omega_v^2 - \omega^2\right) = 0 \quad (32)$$

where

$$\omega_u = \sqrt{\frac{k_u}{m}}$$
$$\omega_v = \sqrt{\frac{k_v}{m}} \quad (33)$$

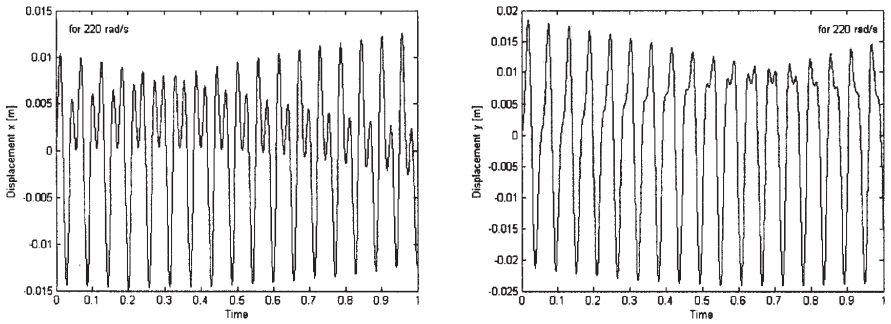

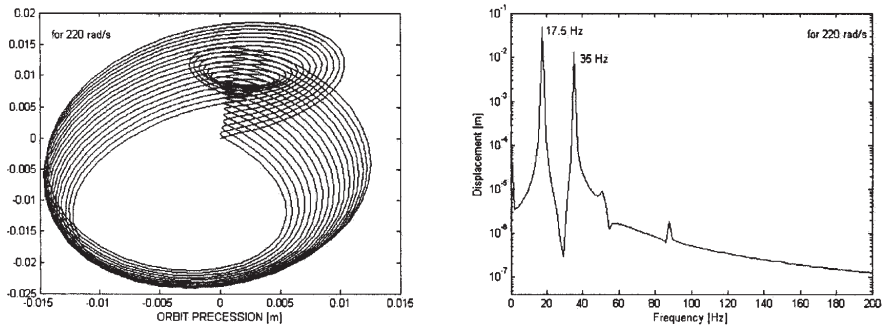

Fig. 5. Simulation results obtained for ω = 220 rad/s compared to the fixed frame

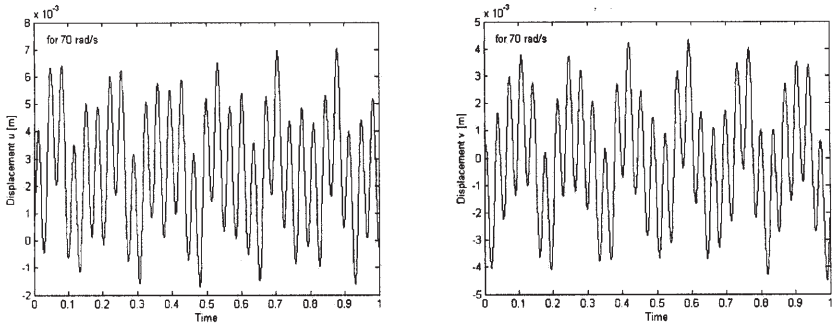

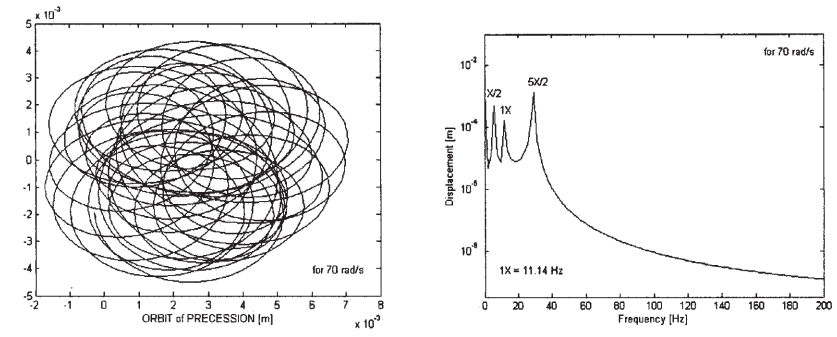

Fig. 6. Simulation results obtained for ω = 70 rad/s compared to the rotated frame

The roots of the equation (32) are:

$$2r_1^2 = -\left(\omega_u^2 + \omega_v^2 + 2\omega^2\right) + \sqrt{\left(\omega_u^2 + \omega_v^2 + 2\omega^2\right)^2 - 4\left(\omega_u^2 - \omega^2\right)\left(\omega_v^2 - \omega^2\right)}$$
$$2r_2^2 = -\left(\omega_u^2 + \omega_v^2 + 2\omega^2\right) - \sqrt{\left(\omega_u^2 + \omega_v^2 + 2\omega^2\right)^2 - 4\left(\omega_u^2 - \omega^2\right)\left(\omega_v^2 - \omega^2\right)} \quad (34)$$

Note that the expression under the radical is always positive:

$$\Delta = \left(\omega_u^2 - \omega_v^2\right)^2 + 8\omega^2\left(\omega_u^2 + \omega_v^2\right) > 0 \quad (35)$$

and so, the roots r_1^2 and r_2^2 are always real numbers. But if $\omega_u < \omega < \omega_v$ then always the product $\left(\omega_u^2 - \omega^2\right)\left(\omega_v^2 - \omega^2\right) < 0$ and $r_1^2 > 0$. Be $r_1^2 = a$, so $r_{1,1} = -\sqrt{a}$, so $r_{1,1} = -\sqrt{a}$, $r_{1,2} = +\sqrt{a}$ and taking into account the relationship (31) it follows that, for this range of the pulsation ω, the system has an increasing solution over the time, becoming unstable.

Numerical simulation

To determine the dynamic properties (the orbits of the precession movement, the frequency response curve, finding the range of the instability etc.) of the system as a Jeffcott rotor, made of an orthotropic material, we performed a numerical simulation, for which we used the following inputs: shaft diameter and length are d = 0.03 m, l = 1 m; mass m = 1 kg, with eccentricity e = 0.005 m, is located midway between the bearings, which were considered rigid; elasticity modules have values

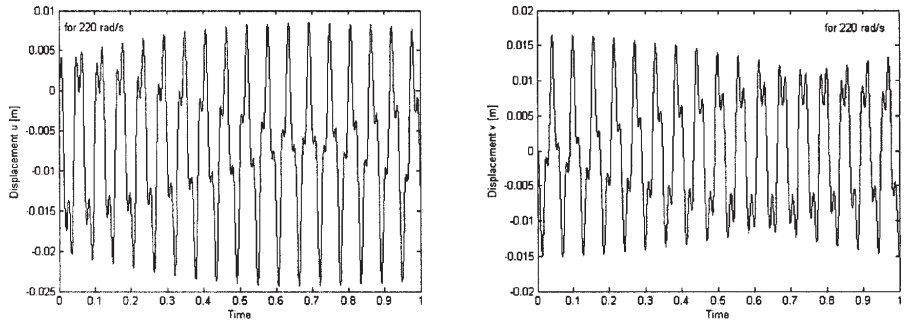

Fig. 7. The simulation results obtained for ω = 220 rad/s compared to the rotated frame

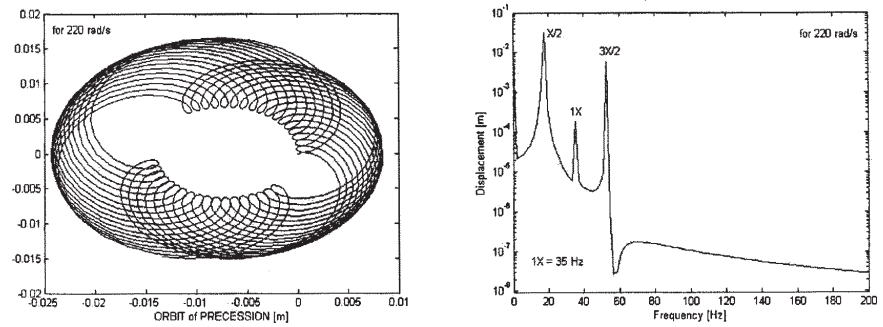

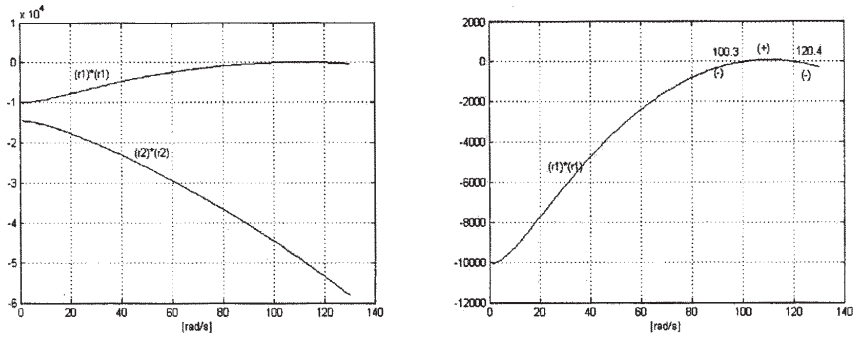

Fig. 8 Finding the unstable range

corresponding to the two directions E_u = 7.6054x10^9 N/m, E_v = 5.2816 x 10^9 N/m. Considering the relations (2) and (33), we obtain two eigenvalues ω_u = 120.4 rad/s and ω_v = 100.3 rad/s, the irrespective natural frequencies f_u = 19.1 Hz and f_v = 15.9 Hz and the critical speed of the rotor ω_{cr1} = 954 rpm and ω_{cr2} = 1146 rpm. Numerical simulations were performed for three different speeds corresponding to three precession frequencies located in three areas of the range of values $\omega_1 < \omega_{cr1} < \omega_2 < \omega_{cr2} < \omega_3$. For all simulations we considered the following initial conditions $[x, y, \dot{x}, \dot{y}] = [0,0,0.3,0.25]$.

Both for the fixed reference system and for the mobile one, numerical simulations were performed at the angular velocities ω_1 = 70 rad/s, ω_2 = 110 rad/s and ω_3 = 220 rad/s. The results are shown in figures 3-7 as it follows: figures 3, 4 and 5 correspond to the fixed reference system, and figures 6 and 7 to the mobile reference system; in all these figures, those marked with a) and b) show the displacement of the centre cross section of the shaft against the time variation, in the right mass m, corresponding to the two axes, $x = x(t)$, $y = y(t)$ and that $u = u(t)$, $v = v(t)$; in figures denoted by c) is given the orbit precession motion obtained by composing the two movements, namely $y = y(x)$ and $v = v(u)$; figures denoted by d) are the Frequency Response Curve and they result from applying the Fast Fourier Transform (FFT) on the data $x + y = x(t) + y(t)$ and $u + v = u(t) + v(t)$. For figures denoted by d) was used, for displacement, representation on a logarithmic axis. Figure 8 summarizes the variations of the solutions $r_1^2 = r_1^2(\omega)$ and $r_2^2 = r_2^2(\omega)$ depending on the angular velocity of the shaft, according to equations (34). While $r_2^2 < 0$ for any value of the pulsation ω, figure 8 - a), r_1^2 is positive when $\omega_{cr1} < \omega < \omega_{cr2}$, figure 8 - b), case in which the system is unstable, the amplitude of the motion grows exponentially in time, according to the equation (31).

Conclusions

The Jeffcott rotor type behaviour, whose shaft is made of an orthotropic material, is totally different from the one whose shaft is made of a material isotropic - case of the circular section steel shaft - and it came to the dynamic behaviour of the rotor with an asymmetric cross-section of the shaft [5-7]. In the case of an isotropic material, the orbit precession of the motion has an ellipse shape, stationary as long as the shaft speed is constant [8]. If the material is orthotropic, while speed remains constant, the orbit precession of the movement shows a variety of forms, figures 3-7 c), according to the occurring nonlinear vibrations. The orbits precession of the movement shows finite values as long as the angular velocity of the shaft is not in the area of instability, ω_{cr1} - ω_{cr2} and values that grow exponentially with time,(fig. 4-c), for the unstable area.

And in terms of Frequency Response Curve we noticed differences between fixed coordinate system and the mobile one. Moreover, in both cases, the differences

between a Frequency Response Spectrum of an isotropic shaft, which would have, in this case, due to mass imbalance, only one component (1X, the corresponding shaft speed) and the corresponding orthotropic shaft are significant. Thus, for the fixed coordinate system emerged the following features: if $\omega < \omega_{cr1}$, in the Response Spectrum two components appear, one fixed, independent of speed shaft, corresponding to the arithmetic mean of the two critical angular speeds, $(\omega_{cr1} + \omega_{cr2})/2$, that means 17.5 Hz, and the second variable, depending on the shaft speed (for the considered simulation $\omega = 70$ rad/s, corresponding to the frequency 11.14 Hz; if $\omega_{cr1} < \omega < \omega_{cr2}$ and so the rotor is in the unstable range, in the spectrum there will be only one frequency component corresponding to 17.5 Hz (average of the two critical speeds); if $\omega > \omega_{cr2}$, the spectrum includes, as in the first area, two peaks, one at 17.5 Hz and another one depending on the shaft speed and which, for the considered case, that has the value 35 Hz (fig. 5-d). In the case of the mobile reference system, both in the range $\omega < \omega_{cr1}$, and for $\omega > \omega_{cr2}$, in the Frequency Response Curve there are three components: one corresponding to the shaft speed (denoted by 1X), as well as an over- an under- first harmonic components X/2 and 5X/2, X/2 and 3X/2.

From the above, the results show a totally different dynamic behaviour of the rotor made of an orthotropic material compared with the one made of an isotropic material. The created model and the code written in MATLAB illustrate this.

References

1. AUTAR K., Mechanics of Composite Materials, 2nd ed, CRC.Press. (2005) ISBN 0-8493-1343-0.
2. MORTON, J., HO, H., TSAI, M.Y., FARLEY, G.L., "An Evaluation of the Iosipescu Specimen for Composite Materials Shear Property Measurement," Journal of Composite Materials, Vol 26. No. 5, 1992, p. 708.
3. *** ASTM Practice D 4065, "Determining and Reporting Dynamic Mechanical Properties," AnnualBook of ASTM Standards, Vol 8.02, American Society for Testing and Materials, West Conshohocken, PA.
4. BUZDUGAN, GH., Rezistenţa materialelor, Editura Tehnică, 1970.
5. TAYLOR, H. D., Critical-speed behaviour of unsymmetrical shafts, Journal of Applied Mechanics, June 1940, pp A71-A79.
6. BROSENS, P. J., CRANDALL, S. H., Whirling of unsymmetrical rotors, Journal of Applied Mechanics, Trans.ASME, Series E, Vol.28, no.3, 1961, p. 355-362.
7. GENTA, G., Whirling of unsymmetrical rotors. A finite element approach based on complex coordinates, Journal of Sound and Vibration, Vol.124, no.1, 1988, p. 27-33.
8. RADES, M., Dynamics of machinery,**2**, 1st ed, Ed. Printech, 2009, p. 206-229

Manuscript received: 11.02.2013